

Response to Reviewer #1's Comments:

Jiayi Li et al. (Author)

The manuscript has been substantially improved. My major concerns has been addressed. However, with the inclusion of new material, there are a number of lingering suggestions the authors should consider before their manuscript is accepted for publication. My main concern is on the interpretation of the V shape. Based on the new material, even though the V shape is clear in the analysis, this is not the manifestation of physical processes, instead, the artifact of spatial variability included in the analysis. In other words, in an ideal observational system, where it is possible to compute statistics at domains smaller than 1deg, the V shape disappears.

Response: We sincerely appreciate the reviewer's constructive comments, which have helped us improve the manuscript and clarify the interpretation of the V shape. In general, we agree with the reviewer that the V shape is an artifact of spatial variability in the ECS region rather than a robust physical signal.

As detailed in our responses to Comments #8 to #10, we have: (a) explicitly discussed the potential influence of spatial sampling inhomogeneity, (b) revised the relevant sections to avoid over-interpretation of the V shape, and (c) toned down any claims that could imply it is a genuine physical feature.

We believe these revisions make the interpretation more cautious and consistent with the limitations of the current observational configuration. Further investigations with sub-degree spatial sampling would indeed be valuable and are now mentioned as a future research direction.

Below, we provide a point-by-point response in blue. The changes to the text are highlighted in red. A version of the revised manuscript with tracked changes is also provided.

1. Line 11: "geostationary observations were conducted"? you mean "Himawari-8 retrievals were used to investigate ACI in 2 regions"?

Response: The reviewer's interpretation is correct. We have rephrased the sentence as suggested.

2. Line 15: "...is driven primarily by diurnal-related boundary layer decoupling and cloud top entrainment" Since the entrainment was not directly estimated, the statement is speculative and should be modified accordingly.

Response: Thank you for your careful review. We have rephrased the sentence to be more accurate (see Lines 16-17): "Furthermore, the diurnal variation of LWP adjustments is likely driven by cloud-top entrainment in the ECS region, but is primarily associated with diurnal-related boundary layer

decoupling in the AUW region.”.

3. Line 32: The Albrecht 1989 citation is incorrect in the context of the sentence.

Response: We thank the reviewer for this comment. The Albrecht 1989 citation is for the precipitation suppression due to life time effect. We have rephrased the sentence to be more accurate (see Lines 31-32): “For example, it has been documented that liquid water path (LWP) can either increase (positive LWP adjustments) due to precipitation suppression (Albrecht, 1989).”.

4. Line 34: “...as the least understood...” the phrase is not needed.

Response: Thank you for your comment. We have removed the phrase.

5. Line54-61. Qiu et al. (2024) needs to be described here because the paragraph is misleading.

Response: We appreciate the reviewer for this insightful comment. We have rephrased the paragraph as suggested (see Lines 54-66): “To date, a majority of studies have relied on observations from polar-orbiting satellites to investigate LWP adjustments and cloud microphysical properties (Bennartz and Rausch, 2017; Gryspeerd et al., 2019; Li et al., 2018; McCoy et al., 2018; Rosenfeld et al., 2019), which are insufficient to depict the time-dependent nature of LWP adjustments. Recent studies began to emphasize the diurnal evolutions of LWP adjustments with geostationary satellites. For example, Rahu et al. (2022) detected polluted cloud tracks over Eastern Europe and revealed afternoon LWP increases in some cases. Qiu et al. (2024) identified a distinct “U-shaped” diurnal pattern of LWP adjustments over the Eastern North Atlantic. However, the understanding of diurnal LWP adjustments, particularly their interplay with varying meteorological conditions and boundary layer dynamic mechanisms, remains limited. Based on Himawari-8 geostationary satellite, the diurnal variations of cloud microphysical properties and LWP adjustments in two typical regions, and the associated influencing factors and mechanisms are presented in this study. Our research aims to expand our understanding of the influence of meteorological factors, initial aerosol states (especially N_d), and the covariance between meteorology and aerosols on cloud LWP, gaining a comprehensive understanding of the diurnal variations in LWP adjustments, which is a highly time-dependent variable lacking quantification, in conjunction with shifts in regional meteorological conditions.”.

6. Line 130 where is the $r_e=14$ μm threshold coming from?

Response: Thanks for pointing this out. The $r_e = 14 \mu\text{m}$ threshold is based on Rosenfeld et al. (2012). Their results show that the precipitation intensified quickly when r_e exceeds $14 \mu\text{m}$ ($> 2.5 \text{ mm d}^{-1}$). The threshold has been widely used in satellite-based studies to distinguish between drizzle scenes and non-drizzle scenes (e.g., Gryspeerd et al., 2019; Rosenfeld et al., 2019; Zhou and Feingold,

2023).

We have rephrased the sentence to be more accurate (Lines 132-134): “Considering the limited ability of GPM to detect light precipitation and drizzle, we additionally applied a $r_e = 14 \mu\text{m}$ threshold to distinguish between drizzle scenes and non-drizzle scenes (Rosenfeld et al., 2012)”.

7. Line 145-148. This justification doesn’t make sense. Could you clarify it please?

Response: Thank you for raising this question. We acknowledge that the description is inaccurate. Both equal-sample bins and equal-width bins have been employed in previous studies with comparable results (Fons et al., 2023; Goren et al., 2025; Gryspeerd et al., 2019; Qiu et al., 2024; Rosenfeld et al., 2019; Zhou and Feingold, 2023). Given our substantial sample size (480189 cloud samples in the AUW and 173181 cloud samples in the ECS) and to ensure consistency with the subsequent analysis of joint histograms of N_d and LWP in log-log space, we employed equal-width binning. Specifically, the median LWP within each $\log(N_d)$ bin was used to regress the slope.

We apologize for the misleading and have rephrased the sentence to be more accurate (see Lines 145-149): “Given our substantial sample size and to ensure consistency with the subsequent analysis of the joint histograms of N_d and LWP in log-log space, we employed equal-width binning, using the median LWP within each $\log(N_d)$ bin to regress the slope. To reduce noise from sparse samples, only bins with more than 50 samples were used to calculate LWP adjustments. Additionally, we tested the equal-sample binning method. The patterns of the N_d -LWP relationship and diurnal variations of LWP adjustments remained robust across different binning methods.”.

8. Page 7, first paragraph. The results for ECS do not contradict Gryspeerd et al. (2019). Note that the N_d range in Gryspeerd does not exceed 300 /cc. In contrast Fig 1b depicts datapoints > 300 /cc. And the increase in N_d with LWP in SatCORPS NASA retrievals occur for $N_d > 300$. My interpretation is that the East China Sea region and its range of variability is not represented in previous studies, but, again, I don’t see necessarily a discrepancy. The question is whether this increase in N_d with LWP is also observed in regions over land, where one should expect high N_d values.

Response: We thank the reviewer for this insightful comment. We agree that our results over the ECS region do not contradict previous studies, and the difference is largely due to the sampling range. To elucidate the influence of the N_d range, we selected a polluted continental region in the west of the ECS region, where 46% of samples exhibit $N_d > 300 \text{ cm}^{-3}$, and a pristine oceanic region, with only 5% of high N_d samples (Fig. R1A). The continental region exhibits a general increase in LWP with N_d (Fig. R1B). In contrast, the oceanic region shows a general decrease in LWP with N_d (Fig. R1C). The result demonstrates that the V shape in the ECS region results from the mixing of

continental and oceanic air masses within the coastal zone.

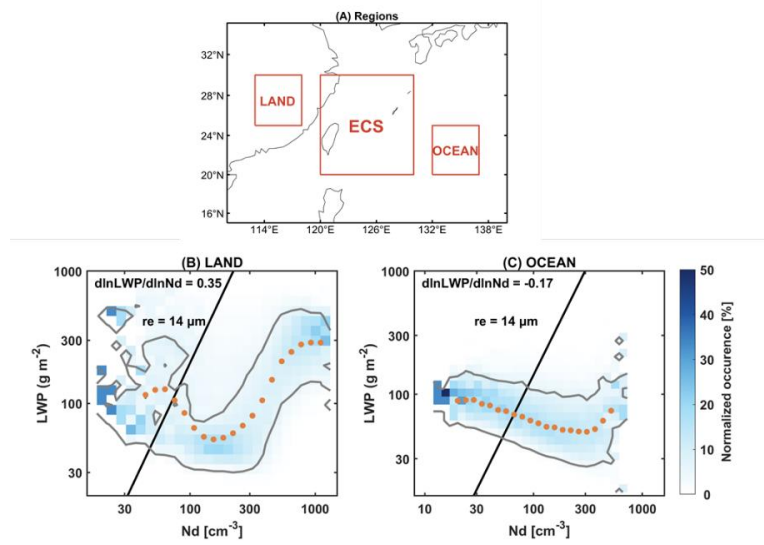


Figure R1: Normalized joint histograms of N_d and LWP for all samples in log-log space (B) in the west land and (C) in the east ocean of the East China Sea. Panel (A) shows the geographical location of the selected regions (ECS: 20°-30°N, 120°-130°E, LAND: 25°-30°N, 113°-118°E, OCEAN: 20°-25°N, 132°-137°E). Orange dots in panels (B) and (C) represent the median LWP in each N_d bins with a sample size greater than 50. The black lines are fitted based on the bins in the joint histogram with the effective radius (r_e) closest to 14 μm . Gray contours indicate 5% occurrence levels. **The figure is the same as Figure S4 in the revised manuscript.**

We have revised the paragraph as suggested (see Lines 198-213): “According to Fig. 1B, LWP begins to rise at high N_d ($> \sim 300 \text{ cm}^{-3}$), exhibiting a V shape that dominates the overall positive LWP adjustments in the ECS region. Although a positive sensitivity of LWP to N_d perturbations has been reported (Bender et al., 2019; Gryspeerd et al., 2019; Michibata et al., 2016; Zhang et al., 2021), its origin remains unclear. To investigate whether the positive N_d -LWP relationship is biased by broken scenes, we assessed the sensitivity of our results to CF. As shown in Fig. S3, the rise in LWP at high N_d coincides with an increase in CF. The average CF for samples with $N_d > 300 \text{ cm}^{-3}$ is 86%. The positive N_d -LWP relationship persists in both overcast (CF $> 80\%$) and broken (CF $< 80\%$) cloud scenes, but the magnitude of the positive adjustment is markedly larger under high-CF scenes. Thus, the LWP rise at high N_d is unlikely to be an artifact of broken-cloud scenes; rather, overcast environments amplify the positive LWP adjustment.

It is plausible that the unique N_d -LWP relationship over the East China Sea is closely related to heavy pollution advected from the continent. Previous studies of LWP adjustments have typically concentrated on the range of N_d below 300 cm^{-3} . However, 18% of the samples exhibited N_d values exceeding 300 cm^{-3} in the ECS region, where clouds are downwind of the major emission sources of China. We further compare the N_d -LWP relationships over the continental region (46% of

samples have $N_d > 300 \text{ cm}^{-3}$) in the west of ECS and the oceanic region (5% of samples have $N_d > 300 \text{ cm}^{-3}$) in the east of ECS, respectively (Fig. S4). Results demonstrate that LWP generally rose with increasing N_d on the heavily polluted continent, while LWP declined with N_d over the ocean. The opposing N_d -LWP relationships correspond to the ascending and descending branches of the V shape, which indicates that V shape results from mixing samples of continental and oceanic air masses.

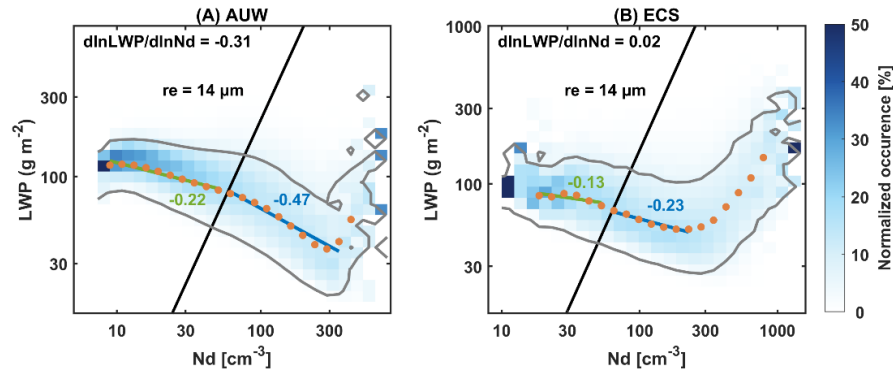


Figure 1: Joint histograms of N_d and LWP in log-log space in the AUW and ECS regions (the west of Australia, AUW and the East China Sea, ECS). The column of each N_d bin is normalized. The black lines are fitted based on the bins in the joint histogram with the effective radius (r_e) closest to $14 \mu\text{m}$. The gray lines represent the contour of 5% occurrence. Orange dots represent the median LWP in each N_d bins with a sample size greater than 50. The green and blue lines are regression slopes for the orange points with r_e above and below $14 \mu\text{m}$, respectively.

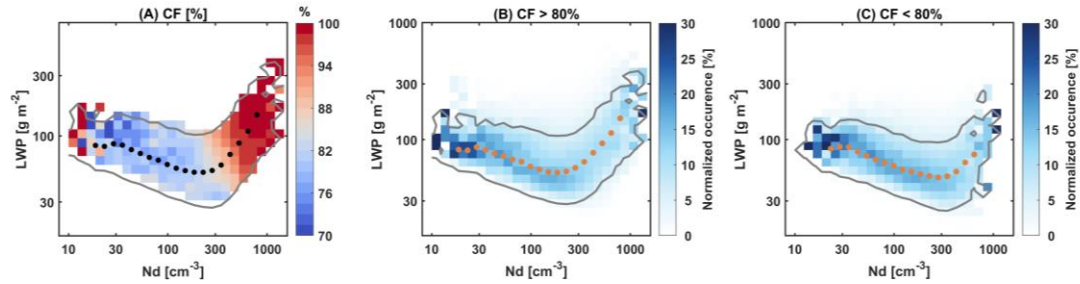


Figure S3: (A) The median cloud fraction (CF) in N_d -LWP log-log space in the ECS region. Only the bins with at least 5% occurrence are shown, bounded by the gray line. Panels (B) and (C) show the normalized joint histograms of N_d and LWP in log-log space in the ECS region, with CF greater than 80% and less than 80%, respectively. Black and orange dots represent the median LWP in each N_d bins with a sample size greater than 50.”.

9. Page 7 second paragraph. Insisting in the same topic of N_d range; it appears plausible that the unique behavior over the East China Sea is contributed by heavy pollution advected from the continent. In other words, meteorology is not the single factors that can modulate the relationship.

Response: Thank you for your comment! As described above in response to Comment #8, we have revised the manuscript to emphasize the impact of N_d range.

10. Figure 2: This is an interesting analysis. It is also relevant because it explains 2 things: 1) The v-shape is the manifestation of spatial variability. In other words, the behavior is the consequence of aggregating data from different locations (Fig. 2a). If the analysis was constrained to a narrower region (e.g. the region west of 124°W), the so called v-shape disappears, and would be replaced by a single regime: a linear increase of N_d with LWP. Second, the linear increase of N_d comes from winter observations (cold SST). All these aspects should be discussed in the paper. Lastly, I would like to emphasize that the v-shape is an artifact, as 2 different sub-domains contribute, individually, to this shape, but in reality, it does not represent the cloud behavior. Having said that, it is still interesting that N_d increases with LWP in winter for coastal clouds. Figure 2 warrants changes to the abstract and the discussion/conclusion section. The importance of this artificial v-shape, attributed to spatial variability, should be deemphasized, while the rather unique increase of N_d with LWP over the East China Sea should be highlighted.

Response: Thank you very much for the constructive comments on our manuscript. We agree with the reviewer that V shape is a result of the spatial variability in the ECS region. Fig. R1 has demonstrated the spatial heterogeneity. Samples in the ECS region are a mixture of continental and oceanic samples. We further performed a sub-domain analysis in the coast and offshore. As shown in Fig. R2, LWP adjustments demonstrate a clear spatial gradient, transitioning from positive values near the coast to negative values offshore. The spatial distribution of LWP adjustments is consistent with N_d . For coastal grids with high N_d values, LWP increases with N_d , particularly after $\sim 300 \text{ cm}^{-3}$ (Fig. R2B), while for offshore grids where N_d values are concentrated below $\sim 300 \text{ cm}^{-3}$, LWP decreases with N_d (Fig. R2C). Therefore, the V shape is the manifestation of spatial variability in the ECS region. We have clarified this in the revised manuscript and, as suggested, provided a more detailed discussion of Figure 2, including the spatial variability and seasonality of the samples (see Lines 224-243): “To further investigate the spatial variability of the ECS region and the potential reasons for the rising behavior of LWP at high N_d , we followed the method of Goren et al. (2025) to present the distribution of environmental conditions in N_d -LWP space (Fig. 2). The cloud samples in the ascending branch are concentrated west of 125°E (Fig. 2A). We performed a sub-domain analysis in the coast and offshore (Fig. S5). LWP adjustments demonstrate a clear spatial gradient, transitioning from positive values near the coast to negative values offshore. The spatial distribution of LWP adjustments is consistent with N_d . For coastal grids with high N_d values, LWP increases with N_d , particularly after $\sim 300 \text{ cm}^{-3}$, while for offshore grids where N_d values are concentrated below $\sim 300 \text{ cm}^{-3}$, LWP decreases with N_d . Therefore, the V shape is the manifestation of spatial variability in the ECS region. The observed increase in LWP at high N_d is attributed to samples from the coastal area. These coastal samples are characterized by cold SST (Fig. 2E), since 75% of the samples are from spring and winter when the Kuroshio Current produces a sharp SST gradient in

the ECS region (Fig. S6) (Liu et al., 2016). Results of summer are statistically insignificant due to the limited samples (3%), particularly after excluding cases with strong precipitation ($GPM = 0 \text{ mm hr}^{-1}$). Such seasonal patterns indicate that the samples are strongly influenced by the northerly cold-air advection at the surface that destabilizes the air-sea interface (Fig. 2, F and G). The potential temperature difference between 950 hPa and 2 m above the sea surface ($\Delta\theta_{950\text{-surf}}$) is calculated as an indicator of sub-cloud layer stability, revealing an extremely unstable sub-cloud layer in the ascending branch (Fig. 2I). Northerly winds transport relatively dry, cold, aerosol-rich air across the warm ocean (Fig. 2, F, G, and H). This destabilizes the sub-cloud layer and intensifies the upward fluxes of sensible and latent heat from sea surface into the atmosphere (Fig. 2, I, J and K) (Long et al., 2020), raising saturation water vapor pressure and facilitating cloud droplet activation. Additionally, high LTS along the coast (Fig. 2L) suppresses the entrainment drying at cloud top (Scott et al., 2020), allowing activated droplets to accumulate more liquid water with thicker clouds (Fig. 2B) and higher CF (Fig. 2C). These conditions jointly elevate both N_d and LWP, resulting in the observed increasing LWP at high N_d .

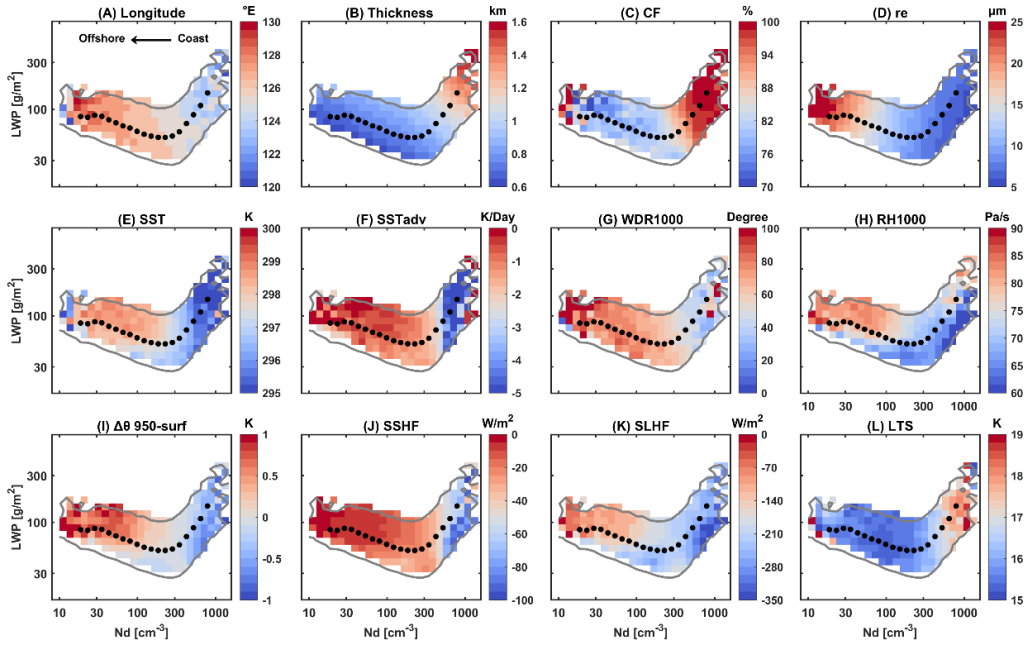


Figure 2: Distributions of meteorological conditions in N_d -LWP log-log space in the ECS region. The color scale represents the median values in each bin. Only bins with an occurrence of at least 5% are shown, bounded by the gray lines. (A) Longitude. (B) Cloud thickness. (C) Cloud fraction (CF). (D) Cloud effective radius (r_e). (E) Sea surface temperature (SST). (F) Horizontal temperature advection at the surface (SST_{adv}). (G) Wind direction on 1000 hPa. 0° indicates a northerly wind. (H) Relative humidity on 1000 hPa (RH1000). (I) The potential temperature difference between 950 hPa and 2 m above the sea surface ($\Delta\theta_{950\text{-surf}}$), a proxy of the sub-cloud layer stability. (J) Surface sensible heat flux (SSHF). (K) Surface latent heat flux (SLHF). For the vertical fluxes, the negative is upwards. (L) Lower-tropospheric stability (LTS). Black dots represent the median LWP in each N_d bins with a sample size greater than 50.

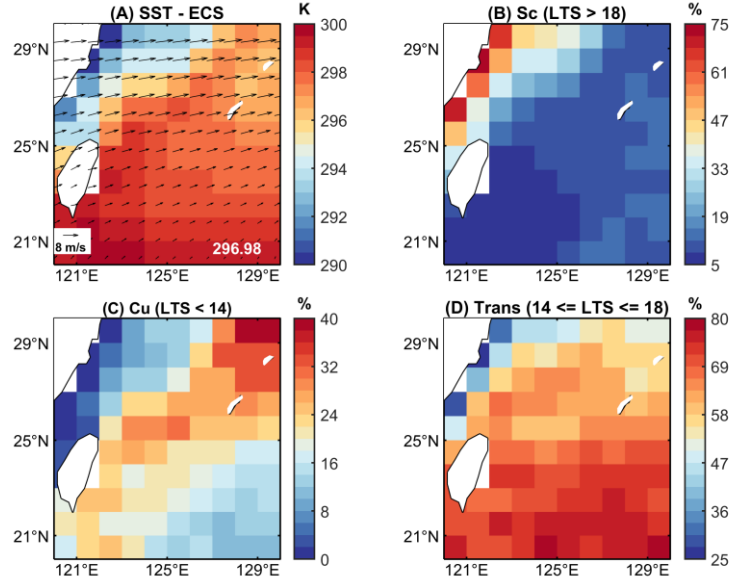


Figure S6: Distributions of meteorological factors and different cloud regimes in the ECS region. (A) Sea Surface Temperature (SST), the composite wind field (arrows) on 700 hPa. The numbers in the lower right corner represent regional averages being weighted by the cosine of latitude. Distributions of the proportion of cloud regimes for (B) Stratocumulus (Sc, LTS > 18 K), (C) Cumulus (Cu, LTS < 14 K), (D) Sc to Cu transition regime (Trans, 14 K <= LTS <= 18 K) are shown.”.

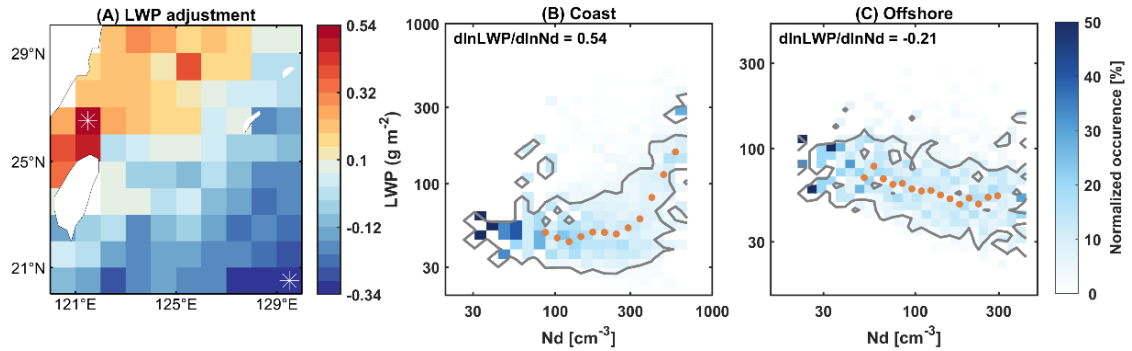


Figure R2: (A) Spatial distribution of LWP adjustments over the ECS region. White asterisks mark the coast and offshore areas for which normalized joint histograms of N_d and LWP in log-log space are presented in panels (B) and (C), respectively. Orange dots in (B) and (C) represent the median LWP in each N_d bins with a sample size greater than 20. Gray contours indicate 5% occurrence levels. **The figure is the same as Figure S5 in the revised manuscript.**

Additionally, we have revised the Abstract and Conclusion sections to deemphasize the V shape and instead highlight the unique positive N_d -LWP relationship found in the coastal region as the key discovery:

Abstract (see Lines 8-21): “Aerosol-cloud interaction (ACI) remains a key uncertainty in climate projections. A major challenge is that the sign and magnitude of cloud liquid water path (LWP)

response to aerosol perturbations (represented by cloud droplet number concentration, N_d) at different temporal and spatial scales are highly variable, but potential microphysical-dynamical mechanisms are still unclear, especially at a diurnal scale. Here, Himawari-8 retrievals were used to investigate LWP adjustments in two distinct cloud regions: the stratocumulus region off the western Australia (AUW) and clouds over the East China Sea (ECS) characterized by a transition from stratocumulus to cumulus under strong anthropogenic influences. In the ECS region, LWP exhibits a unique pronounced rising (positive LWP adjustments) at high N_d . Results indicate that this pattern is driven by northerly cold-air advection during the cold seasons, which enhances surface fluxes and subsequently leads to increases in both LWP and N_d . Furthermore, the diurnal variation of LWP adjustments is likely driven by cloud-top entrainment in the ECS region, but is primarily associated with diurnal-related boundary layer decoupling in the AUW region. The results indicate that neglecting diurnal variations of LWP adjustments leads to an underestimation (up to 89%) of the cooling effect induced by changes in cloud albedo due to aerosol perturbations in the AUW. The bias spans from a 32% overestimation to a 37% underestimation in the ECS. Our findings highlight the key role of diurnal variations of ACI in reducing the uncertainty in climate projections.”.

Conclusion (see Lines 519-528): “In the ECS region, LWP increases at high N_d ($> \sim 300 \text{ cm}^{-3}$), leading to a V shape pattern of N_d -LWP relationship. Our results demonstrate the V shape is the manifestation of spatial variability in the ECS region. Specifically, the ECS serves as a coastal transition zone, experiencing the combined effects of continental and oceanic air masses. Coastal samples show a pronounced LWP increase with N_d , particularly for $N_d > \sim 300 \text{ cm}^{-3}$, while offshore samples exhibit a negative N_d -LWP relationship, with most N_d values below $\sim 300 \text{ cm}^{-3}$. The unique behaviour of LWP increasing at high N_d is attributed to the influence of northerly cold-air advection from the continent during the cold seasons (75% of samples are from spring and winter). The aerosol-rich, relatively cold and dry air from continent reduces the stability of the sub-cloud layer, triggering the release of water vapor into the boundary layer and subsequently promoting cloud droplet activation and development of thicker clouds. These processes collectively lead to an increase in both N_d and LWP, resulting in a positive LWP adjustment at high N_d .”.

11. Page 9, line 244-246. CAO is an extreme manifestation of cold advection, but the idea remains the same, that is, surface fluxes in the cold season are strong, attributed to changes between air-sea temperature differences, which strongly modulate cloud variability.

Response: We appreciate the reviewer’s comment. We have removed the discussion of CAO but emphasized the seasonal pattern of the samples. Specifically, samples from the cold seasons are subject to cold advection, resulting in both increase in LWP and N_d (see Lines 231-236): “The observed increase in LWP at high N_d is attributed to samples from the coastal area. These coastal

samples are characterized by cold SST (Fig. 2E), since 75% of the samples are from spring and winter when the Kuroshio Current produces a sharp SST gradient in the ECS region (Fig. S6) (Liu et al., 2016). Results of summer are statistically insignificant due to the limited samples (3%), particularly after excluding cases with strong precipitation ($GPM = 0 \text{ mm hr}^{-1}$). Such seasonal patterns indicate that the samples are strongly influenced by the northerly cold-air advection at the surface that destabilizes the air-sea interface (Fig. 2, F and G).”.

12. I still find it unnecessary to use cloud thickness to constrain the analysis of LWP. First, as I said in my first review, both LWP and physical depth are functions of optical depth and, therefore, they are not independent variables. Second, there is no physical algorithm for deriving cloud physical depth and, thus, any method is based on empirical relationships, which are highly uncertain. The fact that a remote sensing group provides a product it does not mean that this is suitable for atmospheric research.

Response: Thank you for pointing this out! We acknowledge that cloud thickness (H) should not be used to explain the N_d -LWP relationship, and we have and removed the section using H to constrain the analysis of LWP adjustments.

However, using H to explain the diurnal variation of LWP adjustment is still physically meaningful, especially in the AUW region. H is the result of the boundary layer dynamical condition. Therefore, we emphasize that the different physical processes under differing H conditions determine the diurnal variations of LWP adjustments. Specifically, in the morning thicker clouds occur in a well-mixed boundary layer with stronger cloud-top entrainment and sufficient upward moisture transport (Lu et al., 2023; Zheng et al., 2018b). LWP is less sensitive to entrainment-feedbacks with increasing N_d in thicker clouds. LWP adjustments become more negative with the gradual thinning of clouds. This can be attributed to the weaker moisture transport and cloud-top entrainment in the decoupling boundary layer. As a result, the entrainment feedback with increasing N_d has a greater influence on LWP in thinner clouds, corresponding to more negative LWP adjustments.

Considering H from the passive retrievals has uncertainties, we further perform a validation using the 2B-GEOPROF-LIDAR product from CloudSat-CALIPSO, where H is directly calculated by the cloud base height (CBH) and cloud top height (CTH) of single-layer cloud samples. H from the active sensor was regarded as a reference value of cloud geometrical thickness in previous studies (Zhang et al., 2025) and independent from the passive LWP retrievals. Fig. R3 presents the LWP adjustments across different H bins for the AUW region (2016-2017), derived from collocated pixels of the active satellite product and the geostationary satellite product. The result demonstrates that LWP adjustment increases with H. This finding is consistent with the pattern observed in the manuscript for the AUW region, confirming the robustness of our conclusions.

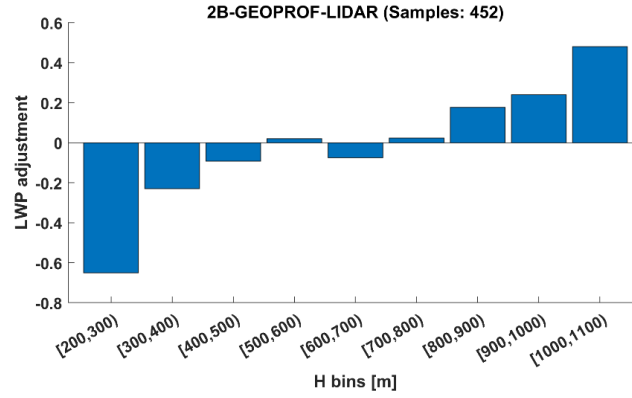


Figure R3: LWP adjustments binned by H for the AUW region (25°-35°S, 95°-105°E) during 2016-2017. H is derived from the CloudSat-CALIPSO 2B-GEOPROF-LIDAR product. LWP adjustment is calculated by the N_d and LWP obtained from the CER_GEO_ED4_HIM08_SH_V01.2 product. **The figure is the same as Figure S20 in the revised manuscript.**

Therefore, we have revised the discussion to better reflect this point only in the section of diurnal variation of LWP adjustments (see Lines 328-350): “In the AUW region, the diurnal variations of the overall LWP adjustments (black line in Fig. 3B) and cloud thickness (blue line in Fig. 3B) demonstrate a strong consistency with a turning point at 1300 LT. In the morning, thicker clouds occur in a well-mixed boundary layer with stronger cloud-top entrainment and sufficient upward moisture transport (Lu et al., 2023; Zheng et al., 2018b). Therefore, LWP is less sensitive to entrainment-feedbacks with increasing N_d in thicker clouds. LWP adjustments become more negative with the gradual thinning of clouds. This can be attributed to the weaker moisture transport and cloud-top entrainment in the decoupling boundary layer. As a result, the entrainment feedback with increasing N_d has a greater influence on LWP in thinner clouds, corresponding to more negative LWP adjustments. Qiu et al. (2024) also discovered the important role of thick-thin cloud transitions in the diurnal variation of LWP adjustments. Rosenfeld et al. (2019) pointed out that cloud thickness (H) constrained most of the meteorological impacts, and N_d explained nearly half of the LWP variability for a given H. We further constrain LWP adjustments in different H intervals (Fig. S19B). Negative LWP adjustments become weaker as H increases (Fig. S19B). Our results suggest that the physical processes under different H conditions appear to determine how LWP changes with N_d , rather than H itself.

Rosenfeld et al. (2019) demonstrated an overall positive LWP adjustment when separating H. The discrepancy may arise from their focus on samples in convective cores (top 10% of cloud optical thickness), which are closer to adiabatic, whereas our samples suggest more exchange with the free atmosphere. Considering H from the passive satellite product is based on an empirical relationship, we further validated the conclusion using the 2B-GEOPROF-LIDAR product from CloudSat-CALIPSO, where H is directly calculated by the cloud base height (CBH) and cloud top height

(CTH) of single-layer cloud samples (Fig. S20). The consistent pattern of increasing LWP adjustment with H from both datasets supports the robustness of our conclusion.

In contrast, H cannot explain the diurnal variation of LWP adjustments in the ECS region (Fig. S19E), even when the spatial variability is considered (Fig. S21). This is likely attributed to different cloud regimes and complex meteorological covariations in the ECS region. Therefore, we attempt to explain the diurnal characteristics of LWP adjustments based on the boundary layer mechanisms in the ECS region.

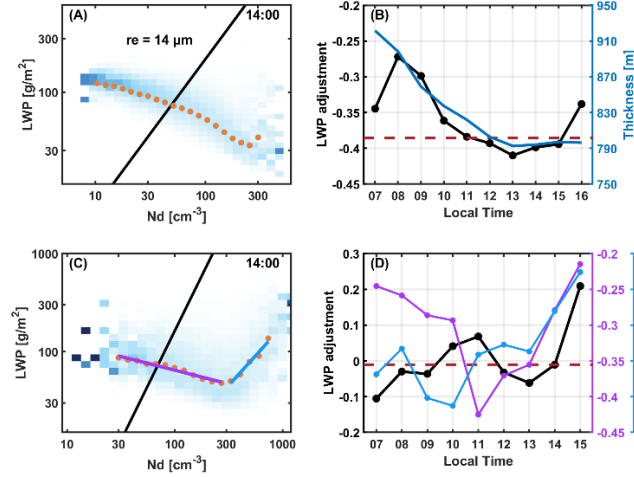


Figure 3: Panels (A) and (C) display the normalized joint histograms of N_d and LWP in log-log space at 1400 LT, for the AUW region and the ECS region, respectively. The complete pictures of all available daytime are presented in Fig. S2. The solid black lines in Panels (B) and (D) show the diurnal variations of LWP adjustments. The blue line in (B) represents the diurnal variation of H in the AUW region. Colored lines in (D) are diurnal variations of different stages in (C). Red dashed lines represent the average LWP adjustments during MODIS Terra (1030 LT) and Aqua (1330 LT) overpasses, -0.39 for the AUW region (B) and -0.01 for the ECS region (D).

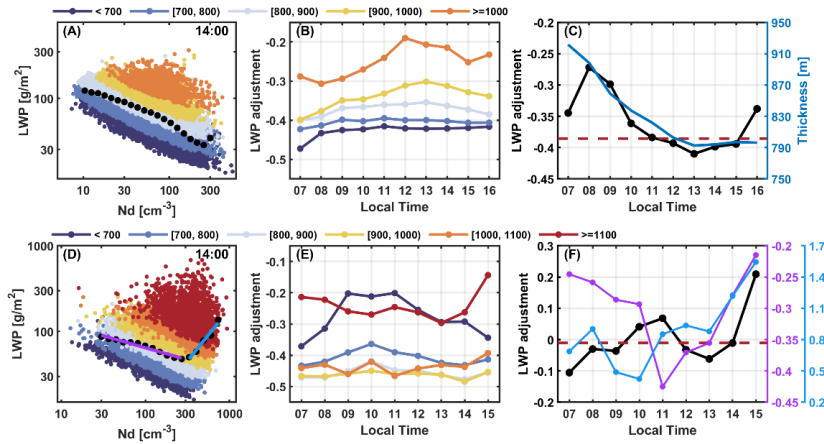


Figure S19: LWP adjustments in log-log spaces and their diurnal patterns in two typical regions. Cloud samples are scattered in N_d -LWP log space at 1400 LT in the (A) AUW and (D) ECS region. The complete pictures of all available daytime are presented in Fig. S11. Colored dots are samples in different

cloud thickness (H) bins (unit: m). Black dots represent the median LWP in each N_d bin. The colored lines are the fits of black dots at different stages in the ECS region. Diurnal variations of LWP adjustments binned by H in the (B) AUW and (E) ECS regions are shown. Colored lines in (F) are diurnal variations of different stages in (D), while black lines in (C) and (F) are the overall diurnal variations of LWP adjustments in two regions, respectively. The blue line in (C) represents the diurnal variation of H. Red dashed lines represent the average LWP adjustments during MODIS Terra (1030 LT) and Aqua (1330 LT) overpasses, -0.39 for the AUW region (C) and -0.01 for the ECS region (F).

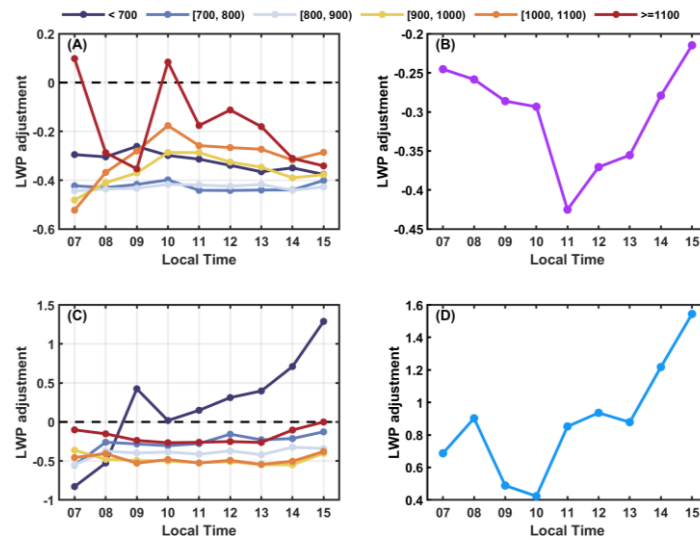


Figure S21: Panels (A) and (C) present the diurnal variations of LWP adjustments binned by H for two different N_d stages of the ECS region in Figure S19D. Panels (B) and (D) display the overall diurnal patterns for the two stages.”.

13. Estimation of cloud height: It suffices to say that the estimation follow the method in Sun-Mack et al (2014).

Response: Thanks for your comment! We have rephrased the sentence as suggested.

14. Line 329: “indicating that entrainment drying originates from evaporation at the cloud base”. This explanation is unphysical. Moreover, in a mixed-layer model, cloud top entrainment is the strongest during the nighttime, because it is driven by turbulence enhancement.

Response: Thank you for your feedback. We acknowledge that attributing the lifting of cloud base to entrainment drying was unphysical. According to the model study by Bougeault (1985), the daytime rise in cloud base height of marine stratocumulus is due to the reduced moisture supply from the surface, resulting from boundary layer decoupling.

The sentence has been rephrased to be more accurate (see Lines 293-295): “The decrease of LWP before 1300 LT is primarily attributed to the lifting of the cloud base, indicating that the upward moisture transport is suppressed, which is in line with an early modeling study for typical Sc cloud

regimes (Bougeault, 1985).”.

15. Line 369, why should we expect a diurnal cycle in subsidence over the open ocean? It doesn't seem realistic. Even if a diurnal cycle in subsidence was observed, it remains to be demonstrated that is meaningful or physical. I am not aware of any large-scale diurnal cycle in subsidence other than in coastal regions near mountainous terrain (e.g. west coast of South America).

Response: We agree with the reviewer's comment. Analysis of ERA5 reanalysis data for the AUW region reveals a weak diurnal variation in the large-scale subsidence (~ 0.047 to ~ 0.054 Pa/s, Fig R4A). Therefore, discussing diurnal variations in this parameter is inappropriate. We have rephrased the sentences in the revised manuscript (see Lines 320-323): “Furthermore, according to the relationship between CLTH, large-scale subsidence (w_s , always negative), and entrainment rate (w_e) ($\frac{dCLTH}{dt} = w_s + w_e$) in the mixed-layer model framework (Painemal et al., 2013), we explain the variations after 1200 LT. Given the weak diurnal variation of w_s over the open ocean (~ 0.047 to ~ 0.054 Pa/s, gray line in Fig 4A), the observed decrease in CLTH after 1200 LT is likely attributed to a weakening of w_e .”.

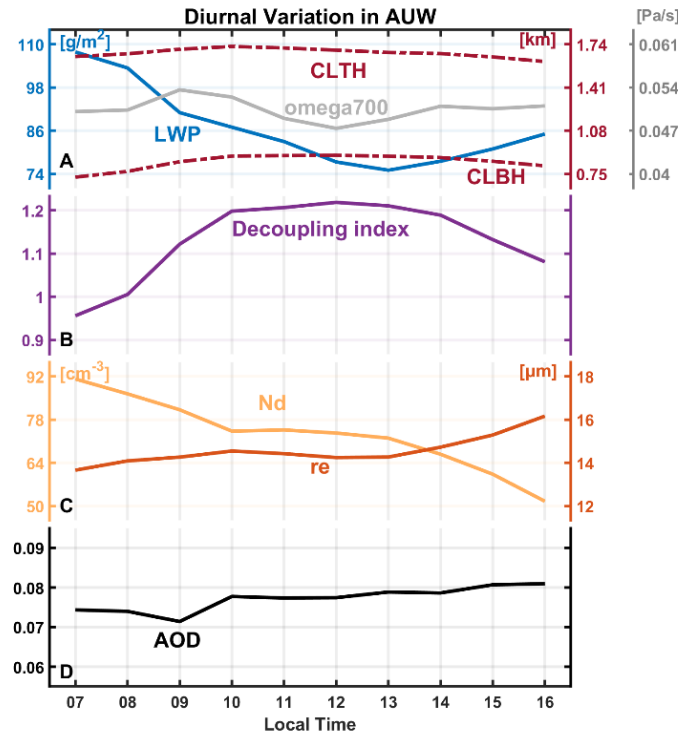


Figure R4: Diurnal patterns in the AUW region. (A) Cloud liquid water path (LWP), cloud-top height (CLTH), cloud base height (CLBH), and vertical velocity on 700 hPa (ω_{700} , positive values indicate downdraft) from ERA5 reanalysis. (B) Decoupling index in the AUW region. (C) Cloud droplet number concentration (N_d) and effective radius (r_e). (D) Aerosol optical depth (AOD). **The figures are the same as Figure 4 in the revised manuscript.**

16. Line 364: It should read “Meanwhile, the decoupling cuts off moisture...”

Response: Thanks for your careful review. We have rephrased the sentence as suggested.

17. Line 387-388: “Apparently, LWP skewness is a more appropriate indicator to reflect cumulus coupling in this region”, What is the line of evidence for this?, why did you use the word “apparently”?

Response: Thanks for your constructive comment! The ECS region is a Sc-Cu transition region due to the “deepening-warming” process. Under this condition, the boundary layer is never fully coupled but exhibits local cumulus coupling. The formation of Cu beneath the Sc causes a positive skewness of the probability density function (PDF) of LWP (Zheng et al., 2018a). Therefore, LWP skewness serves as a measure of the decoupling degree.

We have removed the word “apparently” and rephrased the sentence to be clearer in Lines 362-368: “Under this condition, MBL is never fully coupled but exhibits local cumulus coupling. According to Zheng et al. (2018), the formation of Cu beneath the Sc will render local coupling by feeding moisture into the upper cloud layer, thus causing a positive skewness of the probability density function (PDF) of LWP. Therefore, the skewness of the LWP PDF can be used to estimate the cumulus coupling in this region:

$$\text{skewness} = \frac{E(x - \mu)^3}{\sigma^3} \quad (4)$$

where E is the expected value, μ and σ is the mean and standard deviation of x, respectively. Positive skewness indicates more data tends to be distributed to the right, and vice versa.”.

18. Line 402: “hypothesized” instead of “believed”

Response: The mistake has been corrected.

19. Line 484-486: This is also the conclusion of Qiu et al. (2024)

Response: Thank you for your comments! The sentences have been rephrased in Lines 465-468: “The results highlight the critical need to account for diurnal variations of LWP adjustments when assessing the aerosol indirect effect. This growing consensus among researchers underscores the importance of incorporating geostationary observations or high-resolution simulations to better constrain the diurnal effects of LWP adjustments (Qiu et al., 2024; Rahu et al., 2022; Smalley et al., 2024).”.

20. Line 540: “Cloud thickness in the AUW region serves as a confounder to separate the effects of meteorological covariations.” You have not demonstrated this.

Response: Thanks for your insightful comment! We agree with the reviewer that the statement was not directly demonstrated in our study. We have revised the sentence to maintain accuracy (see Lines 516-517): “Negative LWP adjustments become weaker as cloud thickness increases.”.

21. Line 545: I disagree, Figure 2 clearly shows that the V shape is an artifact of confounding spatial variability with microphysical processes. In other words, the relationship

Response: Thank you for your comment! We noted that the reviewer's final comment appears to be truncated and not fully visible in our system. However, this comment seems to align with the previously raised concerns regarding the V shape. In response, we have revised the sentence to address the concern (see Lines 520-525): “Our results demonstrate the V shape is the manifestation of spatial variability in the ECS region. Specifically, the ECS serves as a coastal transition zone, experiencing the combined effects of continental and oceanic air masses. Coastal samples show a pronounced LWP increase with N_d , particularly for $N_d > \sim 300 \text{ cm}^{-3}$, while offshore samples exhibit a negative N_d -LWP relationship, with most N_d values below $\sim 300 \text{ cm}^{-3}$. The unique behaviour of LWP increasing at high N_d is attributed to the influence of northerly cold-air advection from the continent during the cold seasons (75% of samples are from spring and winter).”.

References

- Albrecht, B. A.: Aerosols, Cloud Microphysics, and Fractional Cloudiness, *Science*, 245, 1227–1230, <https://doi.org/10.1126/science.245.4923.1227>, 1989.
- Bender, F. A.-M., Frey, L., McCoy, D. T., Grosvenor, D. P., and Mohrmann, J. K.: Assessment of aerosol–cloud–radiation correlations in satellite observations, climate models and reanalysis, *Clim Dyn*, 52, 4371–4392, <https://doi.org/10.1007/s00382-018-4384-z>, 2019.
- Bennartz, R. and Rausch, J.: Global and regional estimates of warm cloud droplet number concentration based on 13 years of AQUA-MODIS observations, *Atmos. Chem. Phys.*, 17, 9815–9836, <https://doi.org/10.5194/acp-17-9815-2017>, 2017.
- Bougeault, P.: The Diurnal Cycle of the Marine Stratocumulus Layer: A Higher-Order Model Study, *Journal of the Atmospheric Sciences*, 42, 2826–2843, [https://doi.org/10.1175/1520-0469\(1985\)042%253C2826:TDCOTM%253E2.0.CO;2](https://doi.org/10.1175/1520-0469(1985)042%253C2826:TDCOTM%253E2.0.CO;2), 1985.
- Fons, E., Runge, J., Neubauer, D., and Lohmann, U.: Stratocumulus adjustments to aerosol perturbations disentangled with a causal approach, *npj Clim Atmos Sci*, 6, 130, <https://doi.org/10.1038/s41612-023-00452-w>, 2023.
- Goren, T., Choudhury, G., Kretzschmar, J., and McCoy, I.: Co-variability drives the inverted-V sensitivity between liquid water path and droplet concentrations, *Atmospheric Chemistry and Physics*, 25, 3413–3423, <https://doi.org/10.5194/acp-25-3413-2025>, 2025.
- Gryspeerdt, E., Goren, T., Sourdeval, O., Quaas, J., Mülmenstädt, J., Dipu, S., Unglaub, C., Gettelman, A., and Christensen, M.: Constraining the aerosol influence on cloud liquid water path, *Atmos. Chem. Phys.*, 19, 5331–5347, <https://doi.org/10.5194/acp-19-5331-2019>, 2019.
- Li, J., Jian, B., Huang, J., Hu, Y., Zhao, C., Kawamoto, K., Liao, S., and Wu, M.: Long-term variation of cloud droplet number concentrations from space-based Lidar, *Remote Sensing of Environment*, 213, 144–161, <https://doi.org/10.1016/j.rse.2018.05.011>, 2018.
- Liu, J.-W., Xie, S.-P., Yang, S., and Zhang, S.-P.: Low-Cloud Transitions across the Kuroshio Front in the East China Sea, *Journal of Climate*, 29, 4429–4443, <https://doi.org/10.1175/JCLI-D-15-0589.1>, 2016.
- Long, J., Wang, Y., Zhang, S., and Liu, J.: Transition of Low Clouds in the East China Sea and Kuroshio Region in Winter: A Regional Atmospheric Model Study, *Journal of Geophysical Research: Atmospheres*, 125, e2020JD032509, <https://doi.org/10.1029/2020JD032509>, 2020.
- Lu, X., Mao, F., Rosenfeld, D., Zhu, Y., Zang, L., Pan, Z., and Gong, W.: The Temperature Control of Cloud Adiabatic Fraction and Coverage, *Geophysical Research Letters*, 50, e2023GL105831, <https://doi.org/10.1029/2023GL105831>, 2023.
- McCoy, D. T., Bender, F. A.-M., Grosvenor, D. P., Mohrmann, J. K., Hartmann, D. L., Wood, R., and Field, P. R.: Predicting decadal trends in cloud droplet number concentration using reanalysis and satellite data, *Atmos. Chem. Phys.*, 18, 2035–2047, <https://doi.org/10.5194/acp-18-2035-2018>, 2018.
- Michibata, T., Suzuki, K., Sato, Y., and Takemura, T.: The source of discrepancies in aerosol–cloud–precipitation interactions between GCM and A-Train retrievals, *Atmos. Chem. Phys.*, 16, 15413–15424, <https://doi.org/10.5194/acp-16-15413-2016>, 2016.

Painemal, D., Minnis, P., and O'Neill, L.: The Diurnal Cycle of Cloud-Top Height and Cloud Cover over the Southeastern Pacific as Observed by GOES-10, *Journal of the Atmospheric Sciences*, 70, 2393–2408, <https://doi.org/10.1175/JAS-D-12-0325.1>, 2013.

Qiu, S., Zheng, X., Painemal, D., Terai, C. R., and Zhou, X.: Daytime variation in the aerosol indirect effect for warm marine boundary layer clouds in the eastern North Atlantic, *Atmospheric Chemistry and Physics*, 24, 2913–2935, <https://doi.org/10.5194/acp-24-2913-2024>, 2024.

Rahu, J., Trofimov, H., Post, P., and Toll, V.: Diurnal Evolution of Cloud Water Responses to Aerosols, *JGR Atmospheres*, 127, <https://doi.org/10.1029/2021JD035091>, 2022.

Rosenfeld, D., Wang, H., and Rasch, P. J.: The roles of cloud drop effective radius and LWP in determining rain properties in marine stratocumulus, *Geophysical Research Letters*, 39, <https://doi.org/10.1029/2012GL052028>, 2012.

Rosenfeld, D., Zhu, Y., Wang, M., Zheng, Y., Goren, T., and Yu, S.: Aerosol-driven droplet concentrations dominate coverage and water of oceanic low-level clouds, *Science*, 363, eaav0566, <https://doi.org/10.1126/science.aav0566>, 2019.

Scott, R. C., Myers, T. A., Norris, J. R., Zelinka, M. D., Klein, S. A., Sun, M., and Doelling, D. R.: Observed Sensitivity of Low-Cloud Radiative Effects to Meteorological Perturbations over the Global Oceans, *Journal of Climate*, 33, 7717–7734, <https://doi.org/10.1175/JCLI-D-19-1028.1>, 2020.

Smalley, K. M., Lebsock, M. D., and Eastman, R.: Diurnal Patterns in the Observed Cloud Liquid Water Path Response to Droplet Number Perturbations, *Geophysical Research Letters*, 51, e2023GL107323, <https://doi.org/10.1029/2023GL107323>, 2024.

Zhang, W., Li, J., Li, J., Xu, S., Zhang, L., Wang, Y., and Huang, J.: Cloud heights retrieval from passive satellite measurements using lapse rate information, *Remote Sensing of Environment*, 319, 114622, <https://doi.org/10.1016/j.rse.2025.114622>, 2025.

Zhang, X., Wang, H., Che, H.-Z., Tan, S.-C., Yao, X.-P., Peng, Y., and Shi, G.-Y.: Radiative forcing of the aerosol-cloud interaction in seriously polluted East China and East China Sea, *Atmospheric Research*, 252, 105405, <https://doi.org/10.1016/j.atmosres.2020.105405>, 2021.

Zheng, Y., Rosenfeld, D., and Li, Z.: Estimating the Decoupling Degree of Subtropical Marine Stratocumulus Decks From Satellite, *Geophysical Research Letters*, 45, 12,560–12,568, <https://doi.org/10.1029/2018GL078382>, 2018a.

Zheng, Y., Rosenfeld, D., and Li, Z.: The Relationships Between Cloud Top Radiative Cooling Rates, Surface Latent Heat Fluxes, and Cloud-Base Heights in Marine Stratocumulus, *Journal of Geophysical Research: Atmospheres*, 123, 11,678–11,690, <https://doi.org/10.1029/2018JD028579>, 2018b.

Zhou, X. and Feingold, G.: Impacts of Mesoscale Cloud Organization on Aerosol-Induced Cloud Water Adjustment and Cloud Brightness, *Geophysical Research Letters*, 50, e2023GL103417, <https://doi.org/10.1029/2023GL103417>, 2023.